Enhanced Reliability Assessment in Distribution Network Planning via Optimal Double Q Strategy with Explicit Topology-Variable Consideration

Jianjian JIANG, Qiang LUO, Zhiheng XU, Hao LI, Chong GAO

Guangdong Power Grid Co., Ltd.Guangdong Province, China

jjj7894562024@163.com

Submitted December 12, 2024 / Accepted February 10, 2025 / Online first March 17, 2025

Abstract. *In the planning of distribution networks, assessing reliability is essential for enhancing network design and selection. This research introduces a new distribution network planning model that aims to balance economic performance and system reliability through a double Q strategy. The model integrates important reliability assessment metrics with the optimized design of the distribution network's topology. To address the computational difficulties associated with traditional power flow calculations in complex network configurations, this study employs a linearized power flow method, which enhances the model's practicality and adaptability. Additionally, recognizing the discrete decision-making aspects of the planning issue, a mixed-integer linear programming model is developed. By utilizing the adaptive ε-constraint method, the study investigates the global Pareto frontier between reliability and cost, offering valuable decision-making support for planners. Results from case studies demonstrate that the proposed method effectively lowers the overall construction and operational costs of the distribution network, albeit with a minor reduction in system reliability.*

Keywords

Reliability assessment, distribution network planning, double Q strategy, linearized power flow method, adaptive ε-constraint

1. Introduction

With the increasing penetration of direct current (DC) distributed generation such as solar photovoltaic generation [1], electric vehicle charging stations [2], and DC data centers [3], as well as DC loads in distribution networks, traditional alternating current distribution network (ACDN) systems are undergoing fundamental changes. While the swift evolution of power electronic devices has made DC distribution network (DCDN) systems more efficient and flexible than traditional AC distribution systems, DC distribution networks are still evolving [4]. Hybrid AC/DC distribution network (ADHDN) systems, where AC and DC components coexist, have emerged as potential solutions to ensure economic and reliable power supply. Therefore, it becomes essential to plan the quantity and distribution of components in distribution networks from a global optimal perspective [5].

In the process of distribution network planning, reliability assessment can provide decision-making basis for the improvement of network structure and scheme selection. However, due to the complexity of reliability assessment process, traditional distribution network planning models generally rely on heuristic algorithms for solving, which often cannot guarantee optimal solutions. Traditional distribution network planning models aim to minimize economic costs while satisfying safety constraints such as node voltage and line current [6]. With the increasing scale of distribution networks and the growing demand for power quality from users, reliability has become a crucial factor to consider in distribution network planning [7]–[9]. Among various techniques, the double Q (quantity and quality) planning technique proposed by H. Lee Willis [10] has gained significant attention for its ability to simultaneously consider the economic and reliability aspects of network planning. Existing research on double Q planning techniques can be systematically organized into three main categories based on the methods employed. In the first category, heuristic optimization algorithms are employed to derive solutions for double Q planning [11]–[15]. In this category, multiple distribution system planning schemes are generated iteratively, and the cost and reliability of each scheme are calculated. These metrics are then used as fitness values to guide the optimization algorithm in finding better solutions. Although this method cannot guarantee global optimality, it effectively addresses the complexity of ADHDN planning. For example, article [14] introduces an innovative hybrid methodology that merges discrete particle swarm optimization with optimal power flow calculations, aiming to address the complexities in siting and sizing distributed generation systems more effectively. This approach is designed to assist utilities in identifying the most advantageous integration points for distributed generation within distribution networks from a vast set of potential configurations. A comprehensive strategy for distribution network expansion is introduced in [15], optimizing grid upgrades and integrating renewable/non-renewable

DOI: 10.13164/re.2025.0050

distributed energy sources while managing uncertainties. The genetic algorithm tackles this planning complexity, enhancing reliability through strategic islanding considerations. The second category involves planning methods that combines analytical optimization with manual adjustments to ensure reliability [16]–[19] Initially, an optimization model without direct reliability considerations is established, which is then transformed into a mixed integer programming problem to obtain an initial solution. Subsequently, weaknesses are identified through reliability assessment, and manual adjustments are made based on expert knowledge to meet reliability requirements. This method relies on expert insights, and the optimality of the results is not verified, making it difficult to achieve a balance between reliability and economic efficiency. Article [17] integrates uncertainty and reliability into distribution network expansion planning with distributed generation, considering various asset installation options. An iterative algorithm generates optimal expansion plans, factoring in demand and renewable energy uncertainties, minimizing total costs through stochastic programming. Article [19] introduces a linear programming model that accurately assesses reliability, accounts for post-fault reconfiguration under operational constraints, and quantifies the impacts of variable demand, distributed generation uncertainty, and protection failures on reliability metrics.

Conventional reliability assessment methods are mostly limited to fixed network structures, relying on exhaustive enumeration or heuristic search to explore planning solutions. This indicates that in practical engineering scenarios, relying solely on these methods makes it challenging to find optimal solutions amidst diverse planning options. To overcome this limitation, the third planning framework innovatively integrates direct topological variability reliability assessment into analytical planning models, aiming to achieve optimal "double Q" (quality and economic efficiency) [20]–[24]. In this framework, reliability is no longer dependent on simulation or statistical analysis of fault modes but is integrated directly into the optimization process as part of the planning model, either as a constraint or an objective function, and solved synchronously with the system planning. After being transformed into mixed-integer programming (MIP) models, the system can directly lead to optimal "double Q" planning strategies, overcoming the limitations of traditional methods and providing a dual guarantee of planning efficiency and effectiveness.

There has been a growing demand for explicit reliability assessment methods due to their unique value in obtaining optimal planning solutions. Article [20] introduces a new, efficient algebraic method for analyzing distribution system reliability without relying on simulations or costly optimizations, improving upon prior non-simulation approaches. Article [21] addresses limitations in traditional reliability assessment of distribution networks by introducing a linear-programming-based method that integrates distribution automation and diverse distributed generations. Through a combination of clustering and scenario-based modeling, a mixed integer linear programming model is formulated with SAIDI as the objective, tested and validated in a 37-node system, marking a step forward in incorporating reliability directly into optimization models. A three-stage hierarchical model to boost DC-microgrid resilience is presented in [22], involving proactive measures for storm preparedness, distribution system operator-led generation scheduling and network adjustments to cut costs, and efficient repair crew allocation to minimize unserved energy, all while respecting microgrid privacy in a competitive market environment. Similarly, a novel mathematical model for multi-stage distribution network expansion planning that accounts for reliability is proposed in [23]. It optimizes substation and branch expansions by minimizing total costs, incorporating a new set of algebraic formulas for the Expected Energy Not Supplied index, explicitly weaving reliability into the planning process. Article [24] presents a novel, computationally efficient linear expressions that assess reliability indices of radial distribution networks, accounting for topology variations. Extended to incorporate renewable distributed generation for load restoration during islanding, it also considers stochasticity in renewable output and load demand, facilitating integration into optimization models for reliable network operation and planning.

Building a distribution network planning model that balances performance and cost-effectiveness ("double Q") faces two major challenges: dealing with the complex constraints of mixed AC/DC power flow and effectively integrating topology-based reliability assessment into the model. Current power flow algorithms, such as decomposition iterations and generalized power flow methods, have been applied in practice but are limited by specific network topologies and are not fully adaptable to the topological variability encountered in planning, particularly in handling reverse power flow, which hinders their direct application in planning models. Therefore, integrating power flow calculations with investment decision-making becomes crucial. At the same time, accurately assessing the reliability of distribution networks is another key issue. Current methods can be categorized into simulation and analytical methods, such as the non-sequential Monte Carlo simulation [25], which can handle complex scenarios but are computationally burdensome and exhibit result fluctuations, often used for post-assessment; analytical methods, while providing stable outputs [26], heavily rely on topology logic and need to consider the impact of VSC on system reliability. These factors collectively increase the difficulty of effectively integrating reliability with topological variables, limiting the depth of integration between planning and reliability assessment.

The current body of research indicates that contemporary power system planning models exhibit significant limitations. Primarily, many studies tend to concentrate on unidimensional optimization criteria, such as economic efficiency or reliability, without sufficiently incorporating the reliability assessment of network topology into the planning framework. This gap may result in an inadequate evaluation of overall system performance and the associated risks in real-world applications. Furthermore, the ma-

Ref No.	Objective type	Reliability assessment	Technique
[7–9]	Single objective	Simulation	Mathematical programming
[14]	Single objective	Enumeration-based formulation	Heuristic optimization algorithms
[15]	Single objective	Enumeration-based formulation	Heuristic optimization algorithms
[17], [19]	Single objective	Simulation	Iterative algorithm
[20–24]	Single objective	Non-enumeration-based formulation	Mathematical programming
This study	Dual objectives	Non-enumeration-based formulation	Optimal double Q Strategy

Tab. 1. Comparison of models between related studies and this paper.

jority of existing research does not offer optimization methodologies that can dynamically adjust to fluctuating operational conditions, particularly in light of rapidly evolving load demands and the integration of distributed energy resources. Static planning methodologies are often ill-equipped to provide the necessary flexibility and responsiveness demanded by modern power systems.

Comparison of models between related studies and this paper is displayed in Tab. 1. In response to the identified challenges, this study introduces an adaptive planning model for AC/DC hybrid distribution networks that leverages double Q technology to balance economic efficiency and reliability, integrating network topology reliability assessment with power flow analysis:

- The model incorporates reliability evaluation as a core component, using reliability metrics as constraints and optimization objectives to enhance planning.
- A universal linear power flow algorithm applicable to various topological configurations, including reverse power flow scenarios, is proposed to facilitate accurate analysis.
- Through linearization techniques, the model reformulates complex assessments into a mixed-integer linear programming problem, employing adaptive ε-constraint technology to generate an optimal Pareto frontier for decision support.

The rest of this paper is organized as follows. Section 2 delves into the mathematical modeling of the distribution network planning problem. Section 3 presents the solution method. Section 4 provides a comprehensive case study. Section 5 offers conclusions.

2. Mathematical Modeling of Distribution Network Planning Problem

The evolving trends in future energy systems necessitate a comprehensive consideration of diverse distributed generation (DG) sources and emerging loads, such as wind and solar power generation, as well as energy storage devices, electric vehicle charging infrastructure, and data centers, in the construction of intelligent distribution systems. This imposes higher requirements on distribution system planning. In planning practice, it is essential to intricately design the node layout and line architecture of distribution networks to seamlessly integrate AC and DC power sources and load resources while ensuring a balance between economic efficiency and reliability. Against this backdrop, the planning strategy for ADHDN becomes crucial.

The core lies in coordinating the configuration of AC/DC nodes (depicted by Fig. 1), diverse line deployments, and efficient integration of AC and DC distributed generation resources (ACDG and DCDG) and corresponding loads. Through interconnections between nodes, relying on advanced voltage source converter (VSC) technology, efficient AC-DC energy conversion and dynamic connection are flexibly executed. The internal interconnection system of ADHDN exhibits significant flexibility, mainly manifested in three typical connection modes (illustrated by Fig. 2): direct AC-to-AC connection (Type A), AC-to-DC conversion connection via VSC (Type B), and direct DC-to-DC connection (Type C) [27]. It is noteworthy that although theoretically AC nodes can also be connected via DC lines with VSCs at both ends, this approach was not adopted within the current research framework due to its inferior energy efficiency and economic feasibility. In summary, the planning objective of ADHDN is to establish a highly integrated, energy-efficient, and highly flexible distribution architecture to adapt to and promote the development of future energy systems.

The present study adopts the double Q technique for the planning and construction of hybrid AC/DC distribution networks, aiming to concurrently optimize the cost-effectiveness and high reliability of the distribution system. Within the planning scope of ADHDN, the core tasks are

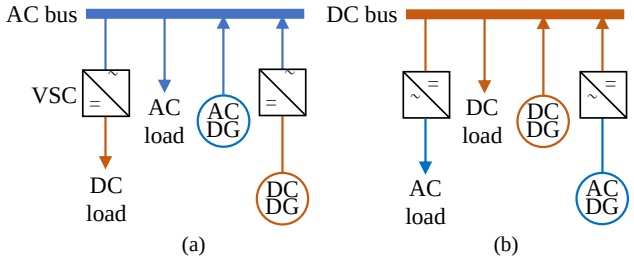

Fig. 1. Configuration of (a) AC bus and (b) DC bus.

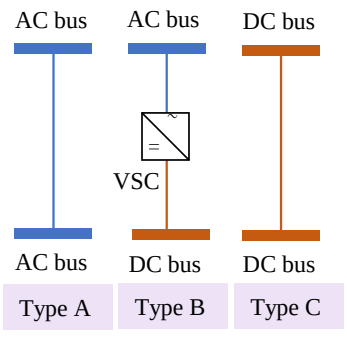

Fig. 2. Three typical connection modes.

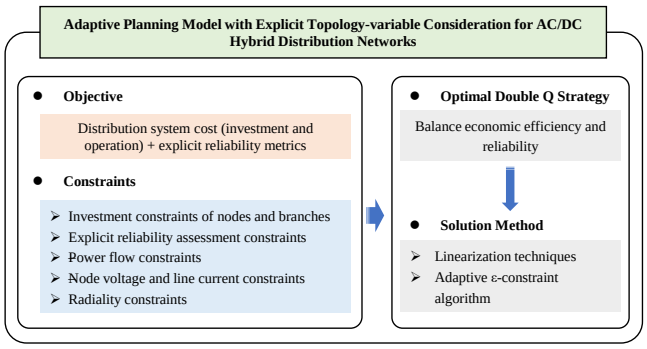

Fig. 3. Framework of the proposed planning model.

subdivided into three main aspects: firstly, defining the operating modes of each node in the system, distinguishing between AC or DC types; secondly, selecting the combinations of lines connecting nodes based on the overall optimization requirements of the system; and finally, determining the technical types of these connecting lines, namely, deciding whether to use AC lines, DC lines, or lines with both AC and DC transmission capabilities. Subsequent sections will elaborate on the objective function of this planning model and the associated constraints involved. The framework of the proposed planning model is illustrated in Fig. 3.

2.1 Objective Function

The planning of hybrid AC/DC distribution systems based on double Q optimization aims to achieve the dual optimization goals of cost and reliability, as shown in (1). The mathematical expression is designed to simultaneously minimize the total cost of the distribution system C^{DN} and the selected reliability metric *RM*. C^{DN} is divided into three main parts: investment cost C^{INV}, operation and maintenance cost C^{MO}, and energy production cost C^{EP}, expressed mathematically as (2). *RM* can be selected from key parameters such as System Average Interruption Duration Index (SAIDI), System Average Interruption Frequency Index (SAIFI), or Expected Energy Not Supplied (EENS), which will be further discussed in the following sections.

$$\min f = \left[C^{\mathrm{DN}}, RM \right], \tag{1}$$

$$C^{\mathrm{DN}} = C^{\mathrm{INV}} + C^{\mathrm{MO}} + C^{\mathrm{EP}}. \tag{2}$$

The total investment cost considers the capital investment in all nodes and branches of the distribution network, as shown in (3). Its mathematical expression reflects the association between each network component and the corresponding investment decision variables: the investment cost at the node level covers the expenses for AC/DC circuit breakers, rectifiers and inverters; while the investment in branches (categorized as type A, B, and C aforementioned) involves the installation cost of the line itself, VSC, and associated circuit breakers. The calculation for maintenance costs (4) is similar to that of investment costs, quantified through corresponding formulas to ensure comprehensive coverage and accurate calculation of system operation and maintenance expenses. As for the generation cost component, it combines the cost of purchasing electricity from the main grid and the net electricity cost generated by distributed generation resources (including both ACDG and DCDG), as computed by (5).

$$\begin{aligned} C^{\mathrm{INV}} = & \sum_{i \in \Omega^{\mathrm{N}}} \left(\mathrm{IC}_i^{\mathrm{NAC}} x_i^{\mathrm{NAC}} + \mathrm{IC}_i^{\mathrm{NDC}} x_i^{\mathrm{NDC}} \right) + \\ & \sum_{b \in \Omega^{\mathrm{B}}} \left(\mathrm{IC}_b^{\mathrm{LA}} z_b^{\mathrm{A}} + \mathrm{IC}_b^{\mathrm{LB}} z_b^{\mathrm{B}} + \mathrm{IC}_b^{\mathrm{LC}} z_b^{\mathrm{C}} \right), \end{aligned} \tag{3}$$

$$\begin{aligned} C^{\mathrm{MO}} = & \sum_{i \in \Omega^{\mathrm{N}}} \left(\mathrm{MC}_i^{\mathrm{NAC}} x_i^{\mathrm{NAC}} + \mathrm{MC}_i^{\mathrm{NDC}} x_i^{\mathrm{NDC}} \right) + \\ & \sum_{b \in \Omega^{\mathrm{B}}} \left(\mathrm{MC}_b^{\mathrm{LA}} z_b^{\mathrm{A}} + \mathrm{MC}_b^{\mathrm{LB}} z_b^{\mathrm{B}} + \mathrm{MC}_b^{\mathrm{LC}} z_b^{\mathrm{C}} \right), \end{aligned} \tag{4}$$

$$C^{\mathrm{EP}} = \hbar \cdot \left(\begin{aligned} & \sum_{s \in \Omega^{\mathrm{NS}}} P_s \cdot Pr + \sum_{i \in \Omega^{\mathrm{ACDG}}} \left(c_i^{\mathrm{ACDG}} - s_i^{\mathrm{ACDG}} \right) P_i + \\ & \sum_{i \in \Omega^{\mathrm{DCDG}}} \left(c_i^{\mathrm{DCDG}} - s_i^{\mathrm{DCDG}} \right) P_i \end{aligned} \right) \tag{5}$$

where x_i^{NAC} and x_i^{NDC} are binary variables indicating whether node i is an AC or DC node. z_b^{A}, z_b^{B} and z_b^{C} are binary variables indicating whether branch b is selected and its type (A, B, or C). $\mathrm{IC}_i^{\mathrm{NAC}}$ and $\mathrm{IC}_i^{\mathrm{NDC}}$ are investment costs for AC and DC nodes. $\mathrm{MC}_i^{(*)}$ (* = NAC and NDC) and $\mathrm{MC}_b^{(**)}$ (** = LA, LB, and, LC) are maintenance costs for corresponding components. h is the weighting factor of the generation cost, it represents the total number of hours in a year (24 hours/day × 365 days/year). Ω^{N}, Ω^{B}, Ω^{NS}, Ω^{ACDG}, and Ω^{DCDG} are the sets of all nodes, all branches, all substations, all ACDG/DCDG connected nodes.

2.2 Constraints

(1) Logical constraints between node and branch investment variables

Building upon the three connectivity modes delineated in Sec. 2.1, a structured set of logical rules is necessitated to govern the interplay between node investment decisions (denoted by variables x_i) and those pertaining to branch investments (represented by z_b). In this context, the symbol "∩" signifies a logical conjunction or "AND" operation, mandating that both implicated conditions hold true for the overall expression to be valid. Conversely, "⊕" denotes the exclusive OR (XOR) operation, yielding truthfulness exclusively when the conditions diverge – one being true while the other false. The specific constraint conditions are as follows: The first condition in (6) establishes that when all connected nodes are AC nodes, type A branches can be activated; the second condition in (6) indicates that the feasibility of type B branches depends on the connected nodes; The third condition in (6) states that type C branches can only be used when the connected nodes are both DC. Particularly, the binary variable z_b associated with any unselected branch b is mandated to assume a value of 0. To rigorously enforce the principle that each branch subscribes to a singular configuration, constraint (7) ensures that if a branch b is indeed selected (as signified by the summation of its type indicators, i.e. y_b

equating to 1), it adheres to a unique typology. Conversely, should the branch remain unchosen (the cumulative sum equating to 0), the specification of its type becomes moot.

$$\begin{cases} 0 \le z_b^{\mathrm{A}} \le \left(x_i^{\mathrm{NAC}} \cap x_j^{\mathrm{NAC}}\right) \\ 0 \le z_b^{\mathrm{B}} \le \left(x_i^{\mathrm{NDC}} \oplus x_j^{\mathrm{NDC}}\right); \forall b \in \Omega^{\mathrm{B}} \\ 0 \le z_b^{\mathrm{C}} \le \left(x_i^{\mathrm{NDC}} \cap x_j^{\mathrm{NDC}}\right) \end{cases} \tag{6}$$

$$y_b = z_b^{\mathrm{A}} + z_b^{\mathrm{B}} + z_b^{\mathrm{C}} \le 1; \forall b \in \Omega^{\mathrm{B}} \tag{7}$$

(2) Explicit reliability assessment based on topological variables

In contrast to preceding reliability investigations that relied on static network configurations, the reliability assessment in the distribution system planning model for ADHDN needs to adapt to the dynamic changes in the network topology. This requires the establishment of a mechanism that directly reflects the mathematical relationship between ADHDN investment decisions and reliability assessment based on topological variables, namely, an explicit reliability assessment method based on topological variables. The significance of VSC failures and their impact on system reliability in ADHDN cannot be ignored in the reliability assessment. Inspired by literature [25], this paper proposes an explicit topological variable reliability assessment method for ADHDN. This paper assumes that faults are caused by specific accidents, covering single-point or multi-point faults. The distribution system operates normally with a radial structure, and distributed generation (DG) supports islanded power supply during faults. The time taken for relay protection is ignored. This assumption is based on the recognition that the relay protection time is much shorter than the equipment repair time, which will be taken into account in future work.

(3) Formulation of EENS

Constraint (8) outlines the calculation of EENS, which integrates the energy losses caused by branch faults $\mathrm{EENS}^{\mathrm{B}}_{k,b}$ and node equipment faults $\mathrm{EENS}^{\mathrm{N}}_{i}$. The energy loss due to branch faults $\mathrm{EENS}^{\mathrm{B}}_{k,b}$ is calculated using (9), where the big M method is employed to automatically adjust the value of $\mathrm{EENS}^{\mathrm{B}}_{k,b}$ based on the selection of branch types. M is a sufficiently large number. Specifically, when a branch is selected, specific conditions are set to calculate the loss, otherwise, the loss is set to zero. When calculating $\mathrm{EENS}^{\mathrm{B}}_{k,b}$, the interruption time $T_b^{\mathrm{repair},k}$ and power reduction P_b^{Curt} for each branch are considered, as shown in (10) and (11), where the interruption time varies depending on the branch type and the impact of VSC on type B branches is taken into account. In (10), $\lambda^{(*)}$ and $\tau^{(*)}$ are failure rate and repair time. Additionally, in (11), based on the islanded operation assumption, if the capacity of DG is sufficient to compensate for the load demand, the power reduction is set to zero; otherwise, it is set to the difference between the demand and the DG capacity, reflecting the contribution of DG to reducing the energy not supplied.

$$\mathrm{EENS} = \sum_{k\in\{A,B,C\}} \sum_{b\in\Omega^{\mathrm{B}}} \mathrm{EENS}^{\mathrm{B}}_{k,b} + \sum_{i\in\Omega^{\mathrm{N}}} \mathrm{EENS}^{\mathrm{N}}_{i}, \tag{8}$$

$$\begin{cases} \left|\mathrm{EENS}^{\mathrm{B}}_{k,b} - T_b^{\mathrm{repair},k} P_b^{\mathrm{Curt}}\right| \le M \cdot \left(1 - z_b^k\right); \forall k \in \{A,B,C\}, \forall b \in \Omega^{\mathrm{B}} \\ \mathrm{EENS}^{\mathrm{B}}_{k,b} \le M \cdot z_b^k \end{cases} \tag{9}$$

$$\begin{cases} T_b^{\mathrm{repair,A}} = \lambda_b^{\mathrm{ACL}} \tau_b^{\mathrm{ACL}} + 2\lambda_b^{\mathrm{ACB}} \tau_b^{\mathrm{ACB}} \\ T_b^{\mathrm{repair,B}} = \begin{pmatrix} \lambda_b^{\mathrm{DCL}} \tau_b^{\mathrm{DCL}} + \lambda_b^{\mathrm{VSC}} \tau_b^{\mathrm{VSC}} + \\ \lambda_b^{\mathrm{ACB}} \tau_b^{\mathrm{ACB}} + 2\lambda_b^{\mathrm{DCB}} \tau_b^{\mathrm{DCB}} \end{pmatrix}; \forall b \in \Omega^{\mathrm{B}}, \\ T_b^{\mathrm{repair,C}} = \lambda_b^{\mathrm{DCL}} \tau_b^{\mathrm{DCL}} + 2\lambda_b^{\mathrm{DCB}} \tau_b^{\mathrm{DCB}} \end{cases} \tag{10}$$

$$P_b^{\mathrm{Curt}} = \begin{cases} D_b^{\mathrm{PD}} - D_b^{\mathrm{DGC}}, D_b^{\mathrm{PD}} > D_b^{\mathrm{DGC}} \\ 0, D_b^{\mathrm{PD}} \le D_b^{\mathrm{DGC}} \end{cases}; \forall b \in \Omega^{\mathrm{B}}. \tag{11}$$

By applying the virtual Kirchhoff's current law (KCL) and considering the power supply and demand at nodes, we compute D_b^{PD} (downstream load demand of the branch) and D_b^{DGC} (downstream available DG power of the branch). Specifically, D_b^{PD} is split into two non-negative parts $D_b^{\mathrm{PD+}}$ and $D_b^{\mathrm{PD-}}$as shown in (12). α_b^{PD} is an auxiliary binary variable. (13) and (14) indicate that the AC/DC load should be converted to match the node type (either the same type as the load node i or AC power for substation node s) to obtain D_b^{PD}. η^{REC} and η^{INV} are conversion efficiencies of the corresponding equipment. $A_{i,b}$ and $A_{s,b}$ are elements of node-branch incidence matrix.

$$\begin{cases} D_b^{\mathrm{PD}} = D_b^{\mathrm{PD+}} + D_b^{\mathrm{PD-}} \\ 0 \le D_b^{\mathrm{PD+}} \le M \cdot \alpha_b^{\mathrm{PD}} \\ 0 \le D_b^{\mathrm{PD-}} \le M \cdot \left(1 - \alpha_b^{\mathrm{PD}}\right) \end{cases}; \forall b \in \Omega^{\mathrm{B}}, \tag{12}$$

$$\sum_{b\in\Omega_s^i} A_{i,b}\left(D_b^{\mathrm{PD+}} - D_b^{\mathrm{PD-}}\right) = x_i^{\mathrm{NDC}}\left(D_i^{\mathrm{AC}} + \eta^{\mathrm{REC}} D_i^{\mathrm{DC}}\right) + \left(1 - x_i^{\mathrm{NDC}}\right)\left(\eta^{\mathrm{INV}} D_i^{\mathrm{AC}} + D_i^{\mathrm{DC}}\right); \forall i \in \Omega^{\mathrm{ND}}, \tag{13}$$

$$\sum_{b\in\Omega_s^S} A_{s,b}\left(D_b^{\mathrm{PD+}} - D_b^{\mathrm{PD-}}\right) = D_s^{\mathrm{AC}} + \eta^{\mathrm{REC}} D_s^{\mathrm{DC}} - G_s^{\mathrm{PD}}; \forall s \in \Omega^{\mathrm{NS}}. \tag{14}$$

Equations (15)–(17) employ similar steps to compute D_b^{DGC}, ensuring consistency with the demand-side calculations. Similarly, D_b^{DGC} is split into two non-negative parts $D_b^{\mathrm{DGC+}}$ and $D_b^{\mathrm{DGC-}}$in (15). α_b^{DGC} is an auxiliary binary variable. (16) and (17) indicate that the AC/DC load should be converted to match the node type (either the same type as the load node i or AC power for substation node s) to obtain D_b^{DGC}.

$$\begin{cases} D_b^{\mathrm{DGC}} = D_b^{\mathrm{DGC+}} + D_b^{\mathrm{DGC-}} \\ 0 \le D_b^{\mathrm{DGC+}} \le M \cdot \alpha_b^{\mathrm{DGC}} \\ 0 \le D_b^{\mathrm{DGC-}} \le M \cdot \left(1 - \alpha_b^{\mathrm{DGC}}\right) \\ D_b^{\mathrm{DGC}} \le M \cdot y_b \end{cases}; \forall b \in \Omega^{\mathrm{B}}, \tag{15}$$

$$\sum_{b\in\Omega_s^z} A_{i,b}\left(D_b^{\mathrm{DGC+}}-D_b^{\mathrm{DGC-}}\right)=x_i^{\mathrm{NDC}}\left(G_i^{\mathrm{ACDG}}+\eta^{\mathrm{REC}}G_i^{\mathrm{DCDG}}\right)+\left(1-x_i^{\mathrm{NDC}}\right)\left(\eta^{\mathrm{INV}}G_i^{\mathrm{ACDG}}+G_i^{\mathrm{DCDG}}\right);\forall i\in\Omega^{\mathrm{ND}}, \tag{16}$$

$$\sum_{b\in\Omega_s^z} A_{s,b}\left(D_b^{\mathrm{DGC+}}-D_b^{\mathrm{DGC-}}\right)=G_s^{\mathrm{ACDG}}+\eta^{\mathrm{INV}}G_s^{\mathrm{DCDG}}-G_s^{\mathrm{DGC}};\forall s\in\Omega^{\mathrm{NS}}. \tag{17}$$

$\mathrm{EENS}_i^{\mathrm{N}}$ is computed by (18), which represents the sum of expected load losses at node *i* caused by the failures of inverters, rectifiers, AC, and DC circuit breakers associated with that node, considering different types of node connections.

$$\mathrm{EENS}_i^{\mathrm{N}}=x_i^{\mathrm{NDC}}\left[\begin{pmatrix}\lambda^{\mathrm{INV}}\tau^{\mathrm{INV}}+\lambda^{\mathrm{ACB}}\tau^{\mathrm{ACB}}+\\ \lambda^{\mathrm{DCB}}\tau^{\mathrm{DCB}}\end{pmatrix}D_i^{\mathrm{AC}}\right]+\left(1-x_i^{\mathrm{NDC}}\right)\left[\begin{pmatrix}\lambda^{\mathrm{REC}}\tau^{\mathrm{REC}}+\lambda^{\mathrm{ACB}}\tau^{\mathrm{ACB}}+\\ \lambda^{\mathrm{DCB}}\tau^{\mathrm{DCB}}\end{pmatrix}D_i^{\mathrm{DC}}\right];\forall i\in\Omega^{\mathrm{N}} \tag{18}$$

(4) Formulation of SAIFI and SAIDI

SAIFI indicates the average number of power interruptions experienced by each customer served by an electric power system within a given time frame. For SAIFI, equation (19) indicates that it includes the number of customer interruptions per year caused by branch *b* failures $\mathrm{SAIFI}_{k,b}^{\mathrm{B}}$ and node *i* failures $\mathrm{SAIFI}_i^{\mathrm{N}}$. (20) and (21) explain how to calculate the number of affected customers N_b^{CurtCus} due to branch *b* failures, based on the comparison between downstream demand D_b^{PD} and available DG power D_b^{DGC}: if DG is sufficient, all customers can be supplied; otherwise, the affected number of customers is calculated proportionally. D_b^{CN} means the customer number of the load points downstream of branch *b*.

$$\mathrm{SAIFI}=\frac{\sum_{k\in\{A,B,C\}}\sum_{b\in\Omega^{\mathrm{B}}}\mathrm{SAIFI}_{k,b}^{\mathrm{B}}+\sum_{i\in\Omega^{\mathrm{N}}}\mathrm{SAIFI}_i^{\mathrm{N}}}{\sum_{i\in\Omega^{\mathrm{N}}}N_i^{\mathrm{Cus}}}, \tag{19}$$

$$\begin{cases}\left|\mathrm{SAIFI}_{k,b}^{\mathrm{B}}-\lambda_{k,b}N_b^{\mathrm{CurtCus}}\right|\le M\cdot\left(1-z_b^k\right)\\ 0\ge\mathrm{SAIFI}_{k,b}^{\mathrm{B}}\le M\cdot z_b^k\end{cases};\forall k\in\{A,B,C\},\forall b\in\Omega^{\mathrm{B}}, \tag{20}$$

$$N_b^{\mathrm{CurtCus}}=\begin{cases}D_b^{\mathrm{CN}}\left(1-D_b^{\mathrm{DGC}}/D_b^{\mathrm{PD}}\right) & ,D_b^{\mathrm{PD}}>D_b^{\mathrm{DGC}}\\ 0 & ,D_b^{\mathrm{PD}}\le D_b^{\mathrm{DGC}}\end{cases};\forall b\in\Omega^{\mathrm{B}} \tag{21}$$

Similar to the computation of D_b^{PD} and D_b^{DGC}, D_b^{CN} is split into two non-negative parts $D_b^{\mathrm{CN+}}$ and $D_b^{\mathrm{CN-}}$, as shown in (22). α_b^{DCN} is an auxiliary binary variable. Equations (23) and (24) indicate that the customer number of the load points downstream of branch *b* should be converted to match the node type (either the same type as the load node *i* or AC power for substation node *s*) to obtain D_b^{CN}.

$$\begin{cases}D_b^{\mathrm{CN}}=D_b^{\mathrm{CN+}}+D_b^{\mathrm{CN-}}\\ 0\le D_b^{\mathrm{CN+}}\le M\cdot\alpha_b^{\mathrm{DCN}}\\ 0\le D_b^{\mathrm{CN-}}\le M\cdot\left(1-\alpha_b^{\mathrm{DCN}}\right)\\ D_b^{\mathrm{CN}}\le M\cdot y_b\end{cases};\forall b\in\Omega^{\mathrm{B}}, \tag{22}$$

$$\sum_{b\in\Omega_B^i} A_{i,b}\left(D_b^{\mathrm{CN+}}-D_b^{\mathrm{CN-}}\right)=N_i^{\mathrm{Cus}};\forall i\in\Omega^{\mathrm{ND}}, \tag{23}$$

$$\sum_{b\in\Omega_B^i} A_{s,b}\left(D_b^{\mathrm{CN+}}-D_b^{\mathrm{CN-}}\right)=N_s^{\mathrm{Cus}}-G_s^{\mathrm{CN}};\forall s\in\Omega^{\mathrm{NS}}. \tag{24}$$

Equation (25) summarizes the total annual customer interruptions due to node *i* associated equipment failures, i.e., $\mathrm{SAIFI}_i^{\mathrm{N}}$, also considering the layout of connected devices at the node. These steps thoroughly assess various aspects of system reliability. λ^{INV}, λ^{ACB}, λ^{DCB}, and λ^{REC} are failure rates of inverter, AC breaker, DC breaker and rectifier connected to the node *i*.

$$\mathrm{SAIFI}_i^{\mathrm{N}}=x_i^{\mathrm{NDC}}\left[\begin{pmatrix}\lambda^{\mathrm{INV}}+\lambda^{\mathrm{ACB}}+\lambda^{\mathrm{DCB}}\end{pmatrix}\mathrm{CN}_i^{\mathrm{AC}}+\lambda^{\mathrm{DCB}}\mathrm{CN}_i^{\mathrm{DC}}\right]+\left(1-x_i^{\mathrm{NDC}}\right)\left[\begin{pmatrix}\lambda^{\mathrm{REC}}+\lambda^{\mathrm{ACB}}+\lambda^{\mathrm{DCB}}\end{pmatrix}\mathrm{CN}_i^{\mathrm{DC}}+\lambda^{\mathrm{ACB}}\mathrm{CN}_i^{\mathrm{AC}}\right];\forall i\in\Omega^{\mathrm{ND}}. \tag{25}$$

SAIDI measures the average duration of power interruptions per customer served by an electric power system over a specified period. Similar to SAIFI, the calculation of SAIDI can be accomplished through (26)–(28).

$$\mathrm{SAIDI}=\frac{\sum_{k\in\{A,B,C\}}\sum_{b\in\Omega^{\mathrm{B}}}\mathrm{SAIDI}_{k,b}^{\mathrm{B}}+\sum_{i\in\Omega^{\mathrm{N}}}\mathrm{SAIDI}_i^{\mathrm{N}}}{\sum_{i\in\Omega^{\mathrm{N}}}N_i^{\mathrm{Cus}}}, \tag{26}$$

$$\begin{cases}\left|\mathrm{SAIDI}_{k,b}^{\mathrm{B}}-T_b^{\mathrm{repair},k}N_b^{\mathrm{CurtCus}}\right|\le M\cdot\left(1-z_b^k\right)\\ 0\le\mathrm{SAIDI}_{k,b}^{\mathrm{B}}\le M\cdot z_b^k\end{cases};\forall k\in\{A,B,C\},\forall b\in\Omega^{\mathrm{B}}, \tag{27}$$

$$\mathrm{SAIDI}_i^{\mathrm{N}}=x_i^{\mathrm{NDC}}\left[\begin{pmatrix}\lambda^{\mathrm{INV}}\tau^{\mathrm{INV}}+\lambda^{\mathrm{ACB}}\tau^{\mathrm{ACB}}+\\ \lambda^{\mathrm{DCB}}\tau^{\mathrm{DCB}}\end{pmatrix}\mathrm{CN}_i^{\mathrm{AC}}+\lambda^{\mathrm{DCB}}\tau^{\mathrm{DCB}}\mathrm{CN}_i^{\mathrm{DC}}\right]+\left(1-x_i^{\mathrm{NDC}}\right)\left[\begin{pmatrix}\lambda^{\mathrm{REC}}\tau^{\mathrm{REC}}+\lambda^{\mathrm{ACB}}\tau^{\mathrm{ACB}}+\\ \lambda^{\mathrm{DCB}}\tau^{\mathrm{DCB}}\end{pmatrix}\mathrm{CN}_i^{\mathrm{DC}}+\lambda^{\mathrm{ACB}}\tau^{\mathrm{ACB}}\mathrm{CN}_i^{\mathrm{AC}}\right];\forall i\in\Omega^{\mathrm{ND}}. \tag{28}$$

(5) Power flow constraints

This study employs a direct current (DC) approximate linear model tailored for ADHDN planning [28]. Below, power flow models will be established for different types of nodes and branches, covering potential occurrences of reverse power flow. Based on Kirchhoff's Voltage Law (KVL), the voltage balance equations for branches are

given by (29)–(31), where the line impedance $Z_b^{(*)}$(*=A,B, and C) is calculated based on the type and length of the branch. (29) and (31) apply to the voltage drops across type A, B, and C branches, while equation (30) is adjusted for type B branches depending on the connected node types. The node voltages V_i are set based on the values of x_i^{NDC}: for DC nodes ($x_i^{\mathrm{NDC}}=1$), V_i is used directly; while for AC nodes ($x_i^{\mathrm{NDC}}=0$), it is represented as V_i/K_cM_c through VSC conversion to denote the DC side voltage. Based on KCL, corresponding equations will be formulated for different types of nodes to provide a detailed analysis of power flow.

$$\left|Z_b^{\mathrm{A}}I_b-\sum_{i\in\Omega^{\mathrm{N}}}A_{i,b}V_i\right|\le M\cdot\left(1-z_b^{\mathrm{A}}\right);\forall b\in\Omega^{\mathrm{B}}, \tag{29}$$

$$\left|Z_b^{\mathrm{B}}I_b-\sum_{i\in\Omega^{\mathrm{N}}}A_{i,b}\left(\frac{V_i}{K_cM_c}+\left(1-\frac{1}{K_cM_c}\right)V_ix_i^{\mathrm{NDC}}\right)\right|\le M\cdot\left(1-z_b^{\mathrm{B}}\right);\forall b\in\Omega^{\mathrm{B}}, \tag{30}$$

$$\left|Z_b^{\mathrm{C}}I_b-\sum_{i\in\Omega^{\mathrm{N}}}A_{i,b}V_i\right|\le M\cdot\left(1-z_b^{\mathrm{C}}\right);\forall b\in\Omega^{\mathrm{B}} \tag{31}$$

where $Z_b^{(*)}$ indicates the line impedance. I means the current through the line and V_i means the voltage at the node. $A_{i,b}$ is the incidence matrix. K_c and M_c are converter constant and modulation index of the converter.

In (32) and (33), positive values represent power injected into node i, while negative values represent power out from node i. They are illustrated by Fig. 4 for better understanding. Constraint (32) ensures the current balance for DC nodes, including the outgoing line currents, DC and AC load consumptions, and the current provided by distributed generation. (33) handles similar considerations for AC nodes, taking into account the current conversion for different types of lines, load demands, and generation inputs, while utilizing the modulation coefficient M_c and constant K_c for voltage conversion through VSC. (34) addresses the specific current outflow situation for AC nodes connected by type B lines. (35) focuses on the current balance for substation nodes.

$$\left|\sum_{b\in\Omega^{\mathrm{B}}}A_{i,b}I_b+\left(\frac{D_i^{\mathrm{DC}}}{V^{\mathrm{DC,r}}}+\frac{D_i^{\mathrm{AC}}}{\eta^{\mathrm{INV}}V^{\mathrm{DC,r}}}\right)-\left(\frac{\eta^{\mathrm{REC}}G_i^{\mathrm{ACDG}}}{V^{\mathrm{DC,r}}}+\frac{G_i^{\mathrm{DCDG}}}{V^{\mathrm{DC,r}}}\right)\right|\le M\cdot\left(1-x_i^{\mathrm{NDC}}\right);\forall i\in\Omega^{\mathrm{ND}}, \tag{32}$$

$$\left|\sum_{b\in\Omega^{\mathrm{B}}}A_{i,b}\left[z_b^{\mathrm{B}}\left(\frac{1}{\sqrt{3}K_cM_c}I_b-I_b\right)+I_b\right]+\left(\frac{D_i^{\mathrm{DC}}}{\sqrt{3}V^{\mathrm{AC,r}}\eta^{\mathrm{REC}}}+\frac{D_i^{\mathrm{AC}}}{\sqrt{3}V^{\mathrm{AC,r}}}\right)-\left(\frac{\eta^{\mathrm{INV}}G_i^{\mathrm{DCDG}}}{\sqrt{3}V^{\mathrm{AC,r}}}+\frac{G_i^{\mathrm{ACDG}}}{\sqrt{3}V^{\mathrm{AC,r}}}\right)\right|\le M\cdot x_i^{\mathrm{NDC}};\forall i\in\Omega^{\mathrm{ND}}, \tag{33}$$

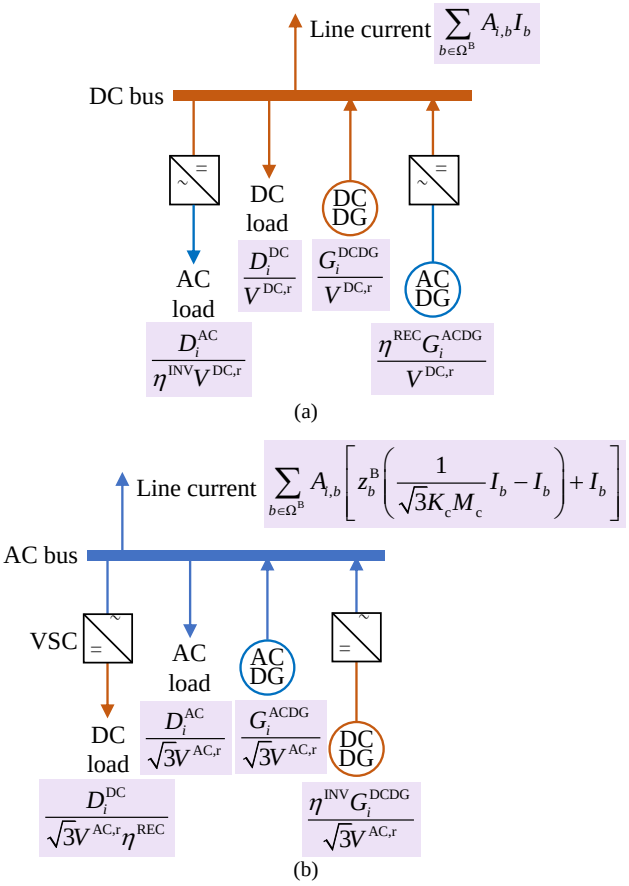

Fig. 4. Illustration of (a) equation (32) and (b) equation (33).

$$I_b=\begin{cases}\dfrac{1}{\eta^{\mathrm{VSC}}I_b}, A_{i,b}I_b\ge 0\\ \eta^{\mathrm{VSC}}I_b, A_{i,b}I_b<0\end{cases};\forall b\in\Omega^{\mathrm{B}}, \tag{34}$$

$$\sum_{b\in\Omega^{\mathrm{B}}}A_{s,b}\left[z_b^BI_b\left(\frac{1}{\sqrt{3}\eta^{\mathrm{VSC}}K_cM_c}-1\right)+I_b\right]+\left(\frac{D_s^{\mathrm{DC}}}{\sqrt{3}\eta^{\mathrm{REC}}V^{\mathrm{AC,r}}}+\frac{D_s^{\mathrm{AC}}}{\sqrt{3}V^{\mathrm{AC,r}}}\right)-\left(\frac{\eta^{\mathrm{INV}}G_i^{\mathrm{DCDG}}}{\sqrt{3}V^{\mathrm{AC,r}}}+\frac{G_i^{\mathrm{ACDG}}}{\sqrt{3}V^{\mathrm{AC,r}}}\right)-\frac{P_s}{\sqrt{3}V^{\mathrm{AC,r}}}=0;\forall s\in\Omega^{\mathrm{NS}} \tag{35}$$

where D_i^{DC} and D_i^{AC} mean the load consumption for DC and AC node, respectively. G_i^{ACDG} and G_i^{DCDG} indicate the generation from AC and DC sources. η is the efficiency factor.

(6) Node voltage and line current constraints

There are constraints on both node voltages and line currents, as described in (36)–(37).

$$\begin{cases}x_i^{\mathrm{NDC}}V_i^{\min}+\left(1-x_i^{\mathrm{NDC}}\right)V_i^{\min}\le V_i\\ V_i\le x_i^{\mathrm{NDC}}V_i^{\max}+\left(1-x_i^{\mathrm{NDC}}\right)V_i^{\min}\end{cases};\forall i\in\Omega^{\mathrm{N}}, \tag{36}$$

$$\left|I_b\right|\le z_b^{\mathrm{A}}I_b^{\max}+\left(z_b^{\mathrm{B}}+z_b^{\mathrm{C}}\right)I_b^{\max};\forall b\in\Omega^{\mathrm{B}} \tag{37}$$

where $V_i^{\min}$ and $V_i^{\max}$ are the minimum and maximum allowable voltages. $I_b^{\max}$ is the maximum allowable current.

(7) Radiality constraints

To guarantee the preservation of a radial configuration in the system, the branching selection process must conform to two essential criteria: firstly, the aggregate count of chosen branches ought to match the overall node count in the system minus the substations' node count, as outlined in (38). Secondly, the maintenance of network connectivity is imperative, a principle that inherently upholds the equilibrium of user numbers, as articulated in (22)–(24).

$$\sum_{b\in\Omega^{\mathrm{B}}} y_b = N - N_s \tag{38}$$

where N and N_{s} represent total number of nodes and the number of substations.

3. Solution Method

The intricacy of the ADHDN planning model is attributed to its thorough incorporation of investment decision variables associated with nodes and branches, alongside node and line type variables. These elements are intricately linked to power flow analysis and system reliability evaluation, thereby significantly complicating the planning problem. Specifically, the dual-objective ADHDN planning framework seeks to minimize direct economic costs while simultaneously maximizing system reliability, resulting in a formidable multi-objective optimization challenge. This complexity is exacerbated when integer variables are involved, as the search for Pareto optimal solutions becomes computationally intensive. Consequently, this paper proposes effective linearization strategies and adaptive ε-constraint algorithms to tackle these intricate challenges.

3.1 Linearization Techniques

The dual-objective ADHDN model, which incorporates non-linear components such as absolute value terms, bilinear terms, logical expressions, and piecewise functions, presents particular difficulties in managing these complex non-linear characteristics. To address this issue, the paper employs a series of linearization techniques that successfully convert the original problem into a solvable MILP framework.

For example, the bilinear term $V_i x_i^{\mathrm{NDC}}$ in (30) is a product of a binary variable and a continuous variable, which can be linearized by introducing auxiliary variables and utilizing the Glover's linearization technique. The linearization formulas are as follows:

$$\begin{cases} V_i^{\min} x_i^{\mathrm{NDC}} \le \delta_i \le V_i^{\max} x_i^{\mathrm{NDC}} \\ V_i - V_i^{\max}\left(1 - x_i^{\mathrm{NDC}}\right) \le \delta_i \le V_i + V_i^{\max}\left(1 - x_i^{\mathrm{NDC}}\right) \end{cases}; \forall i \in \Omega^{\mathrm{N}} \tag{39}$$

3.2 Adaptive ε-constraint Algorithm

Following the linearization process, the dual-objective ADHDN planning model is reformulated into a dual-objective MILP format. As indicated in [29], the application of an adaptive ε-constraint method, which adeptly circumvents redundant optimization steps and efficiently approaches the Pareto frontier, markedly enhances computational efficiency. For the sake of clarity, this paper designates EENS as the primary metric for reliability assessment, while other reliability parameters are incorporated into the problem framework as constraints, thereby streamlining the problem-solving logic. In this method, ε denotes a small positive number that regulates the constraint strictness. By fixing one objective function within a narrow range near its optimum and introducing epsilon, we temporarily exclude it from the multi-objective optimization problem, focusing instead on optimizing the others. Adjusting ε allows us to control solution precision and quantity flexibly, aiding in the discovery of Pareto front points in multi-objective optimization [29].

3.3 Solution Process

The proposed distribution network planning solution framework, based on Double-Q technology, is depicted in Fig. 5. In Fig. 5, "*i*" is an iteration counter, and "*k*" is a scaling factor during the iteration process. "eps" represents epsilon in the adopted adaptive ε-constraint method. This innovative approach synergistically merges cost-effectiveness with the optimization of system reliability. The initial phase employs the lexicon optimization method outlined in [29], creating a profit-oriented table that aims to achieve both the minimization of direct costs and the maximization of system reliability as dual objectives. Subsequently, the step size *d* is established for each iteration. The core algorithm iteratively addresses a series of ADHDN planning problems, prioritizing the direct cost objective for optimization, while treating EENS as an unconstrained constraint to maintain the reliability level of the planning solution. A notable aspect of this process is the implementation of the adaptive ε-constraint method, which skillfully utilizes the coefficient *b* (derived from *s*(*i*)) to eliminate redundant calculations, thereby filtering out unnecessary computational pathways and significantly enhancing the algorithm's computational efficiency and targeting. Through these iterations, the Pareto optimal frontier set is progressively constructed and explored, encompassing all non-dominated trade-off solutions between cost and reliability. Ultimately, utilizing L_p-metric decision theory (as shown in (40)), appropriate compromise solutions are selected from the Pareto frontier set, where the specification of the *p* value directly influences the characteristics of the metric space, thus providing precise guidance for decision-makers in achieving reasonable trade-offs and choices between cost and reliability.

$$L_p = \left[\begin{array}{l} \omega_1 \left| \dfrac{C^{\mathrm{DN}}(i) - C^{\mathrm{DNmin}}}{C^{\mathrm{DNmax}} - C^{\mathrm{DNmin}}} \right|^p + \\ \omega_2 \left| \dfrac{\mathrm{ENSS}(i) - \mathrm{EENS}^{\mathrm{min}}}{\mathrm{EENS}^{\mathrm{max}} - \mathrm{EENS}^{\mathrm{min}}} \right|^p \end{array} \right]^{1/p}, i = 1, 2, \cdots, N_{\mathrm{O}} \quad (40)$$

where ω_1 and ω_2 are weights for cost and reliability.

4. Case Study

In this section, an improved system instance is utilized for analysis, and the detailed structure of the system is depicted in Fig. 6. The test system contains 13 buses and 26 candidate branches. The base AC voltage is set at 4.16 kV, while the DC voltage is 6.8 kV. The AC load for the system is 1.29 MW in total, and the DC load is 1.55 MW. Additionally, the total capacity of ACDG integrated into the system amounts to 0.08 MW, while the total capacity of DCDG is 0.32 MW. Detailed data of line parameters, load and distributed generation capacity are displayed in Tab. 2 and 3. All the numerical tests are performed on MATLAB 2022b with GUROBI 10.0.1 on a personal computer with 16 GB RAM and a 2.30 GHz CPU.

4.1 Results of Different Planning Models

In the comparative evaluation of various distribution system planning models, specifically the purely alternating current distribution network system (ACDN), the purely direct current distribution network system (DCDN), and the ADHDN, the performance of these models was assessed

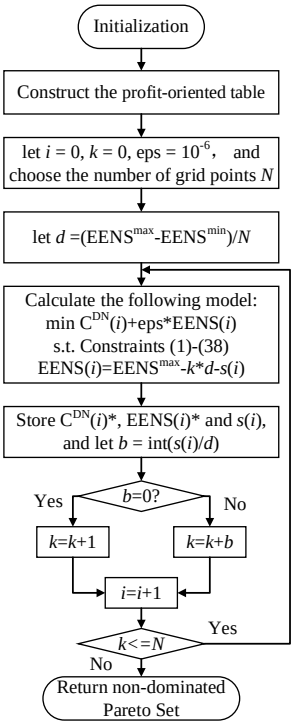

Fig. 5. Flow chart of the solution method.

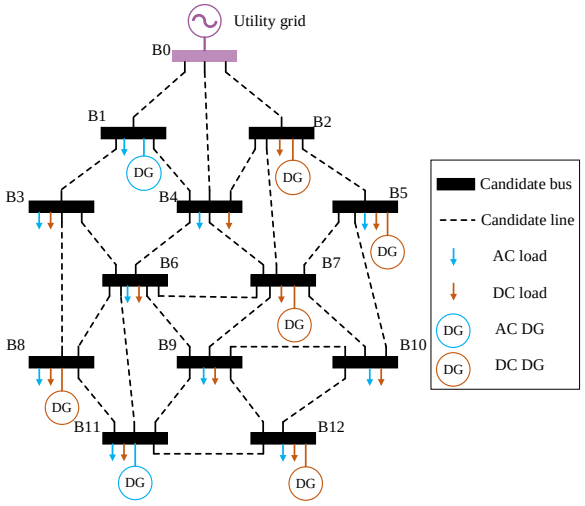

Fig. 6. Topology diagram of the modified 13 buses test system.

through optimization outcomes illustrated by Pareto fronts.These outcomes are graphically represented in Fig. 7, where each point on the Pareto front corresponds to a distribution system configuration that meets optimization criteria concerning cost constraints and reliability standards.

The Pareto front depicted in Fig. 7 clearly indicates that the solution space of ADHDN encompasses the optimal solution sets of both ACDN and DCDN. The ADHDN model exhibited the most extensive range of trade-off options between cost and reliability. This finding provides planners with an enhanced decision-making framework, enabling them to select from a wider array of feasible solutions tailored to specific cost tolerances or reliability requirements.

It should be noted that the stars in Fig. 7 represent the optimal solutions recommended by decision-making techniques. The optimal solution of the DCDN is C^{DN} = 1856.75 k$ and EENS = 47.43 MWh. The optimal solution of the ACDN is C^{DN} = 1850.72 k$ and EENS = 21.6 MWh. The optimal solution of the ADHDN is C^{DN} = 1832.45 k$ and EENS = 25.65 MWh. ACDN demonstrated strong reliability (characterized by low EENS) but incurred substantial costs when incorporating a high proportion of direct current components. Conversely, DCDN exhibited limitations in both economic viability and reliability, primarily due to elevated fault rates and investment costs associated with direct current equipment and VSCs. In contrast, ADHDN identified a more balanced solution. It indicates that the dual-objective ADHDN planning model achieved a more equitable balance between system economy and reliability.

Additionally, Figure 8 presents the optimal solutions (stars in Fig. 7) identified through the three models: ACDN, DCDN, and ADHDN. This study posits that the transition to direct current systems becomes a more rational choice when buses are subjected to significant direct current loads or when there is a higher proportion of direct current distributed generation resources. This suggests that under specific load configurations and resource conditions,

Line No.	First Node	Second Node	Length/km
L1	0	1	1
L2	0	2	1
L3	0	4	1.4
L4	1	3	1.4
L5	1	4	1
L6	2	4	1
L7	2	5	1
L8	2	7	2
L9	3	6	1
L10	3	8	1.4
L11	4	6	1
L12	4	7	1.2
L13	5	7	1
L14	5	10	1.4
L15	6	7	1
L16	6	8	1.2
L17	6	9	1.4
L18	6	11	1.4
L19	7	9	1
L20	7	10	2.2
L21	8	11	1.2
L22	9	10	1.4
L23	9	11	1.4
L24	9	12	1
L25	10	12	1.4
L26	11	12	2

Tab. 2. Line data.

Node	Peak AC load (MW)	Peak DC load (MW)	AC DG capacity (MW)	DC DG capacity (MW)	User number	AC user number	DC user number	Substation node
0	0	0	0	0	0	0	0	1
1	0.22	0	0.04	0	40	40	0	0
2	0	0.27	0	0.04	50	0	50	0
3	0.18	0.09	0	0	46	30	16	0
4	0.22	0.13	0	0	65	45	20	0
5	0.09	0.13	0	0.08	48	18	30	0
6	0.09	0.09	0	0	30	20	10	0
7	0	0.18	0	0.04	40	0	40	0
8	0.13	0.13	0	0.08	55	30	25	0
9	0.09	0.13	0	0	43	18	25	0
10	0.09	0.18	0	0	50	20	30	0
11	0.09	0.09	0.04	0	23	15	8	0
12	0.09	0.13	0	0.08	45	15	30	0

Tab. 3. Data of load and distributed generation capacity.

direct current systems can capitalize on their inherent advantages to enhance overall system economy and adaptability.

4.2 Performance Comparison of Multi-objective Optimization Algorithms

This section undertakes a comparative examination of multiple multi-objective optimization algorithms: NSGA-II [30], the classic ε-constraint methodology [31], and the adaptive ε-constraint approach employed herein. All algorithms underwent evaluation within an identical search grid configuration, with a uniform grid resolution set at $N = 400$ points. A synopsis of the computational outcomes from this algorithmic comparison is presented in Tab. 4. Figure 9 visually demonstrates that NSGA-II yields a smaller quantity of Pareto non-dominated solutions com-

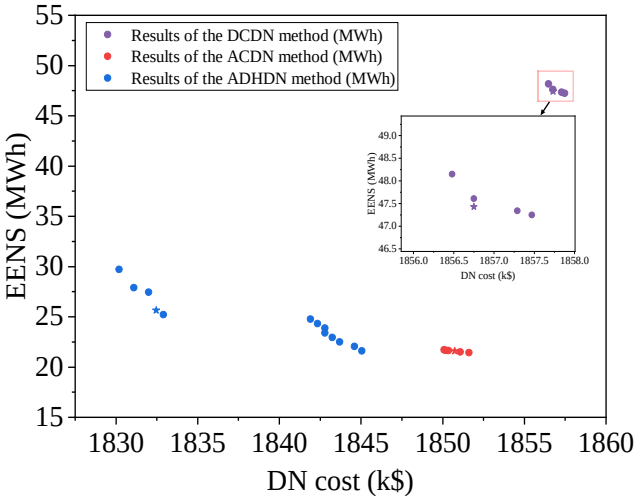

Fig. 7. Results of different planning methods.

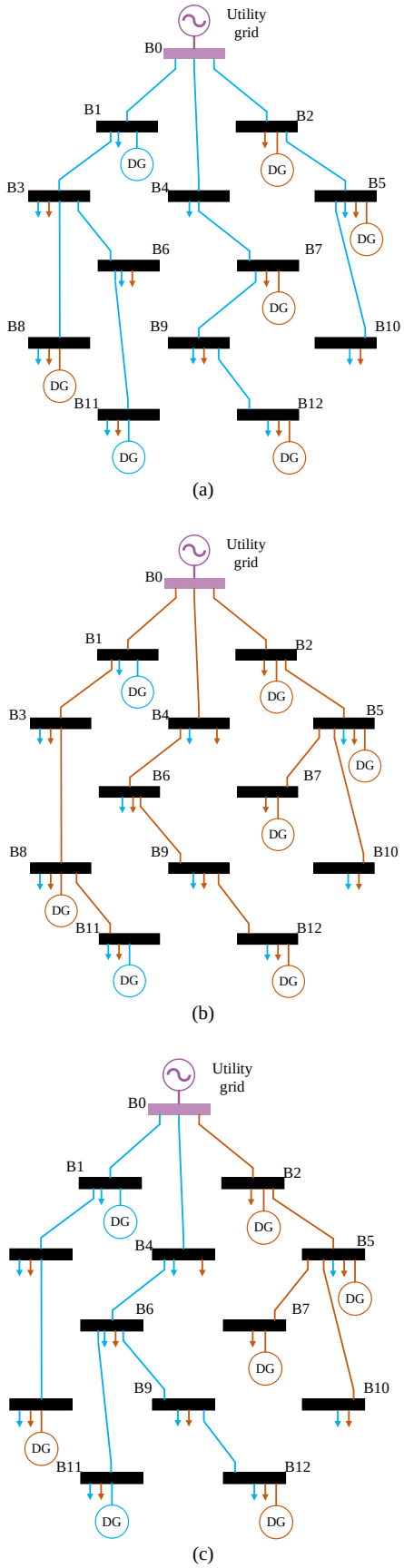

Fig. 8. Optimal distribution network planning schemes of different planning methods. (a) ACDN; (b) DCDN; (c) ACHDN.

pared to the ε-constraint methodologies, and the solutions' overall quality is relatively inferior. The huge number of discrete variables presented in the ADHDN planning model surpasses the capabilities of conventional traversal or heuristic algorithms, such as NSGA-II.

A performance differential threshold of 0% is uniformly implemented across various algorithmic configurations to guarantee the optimality of solutions. The analysis indicates that the optimization objective values obtained through the conventional ε-constraint method are in exact agreement with those derived from the adaptive ε-constraint method, thereby validating the accuracy of both algorithms. However, a critical finding is that the adaptive ε-constraint method significantly reduces the number of iterations required compared to its non-adaptive counterpart. This improvement is attributed to the adaptive ε-constraint method's ability to effectively predict the subsequent Pareto solution candidate through the use of relaxation variables. As a result, this capability substantially lessens the computational requirements for each iteration, thereby expediting the solution process and enhancing overall efficiency.

4.3 Sensitivity Analysis

This section offers a comprehensive examination of the specific effects of DG penetration rates, the proportion of DC components and the failure rate of VSC on the cost and reliability metrics of the distribution system.

Figure 10(a) illustrates a trend of decreasing system costs as the DG penetration rate increases. This phenomenon is primarily attributable to a larger share of the load being managed by local DG, which diminishes dependence on external lines and the need for equipment expansion, thus resulting in cost reductions. Concurrently, the EENS value decreases with rising DG penetration rates, suggesting that the local absorption capacity of DG mitigates load

Methods	#Iter	Time (s)
NSGA-II	400	86383
Traditional ε-constraint method	400	77260
The proposed method	36	54

Tab. 4. Computational results of different algorithms.

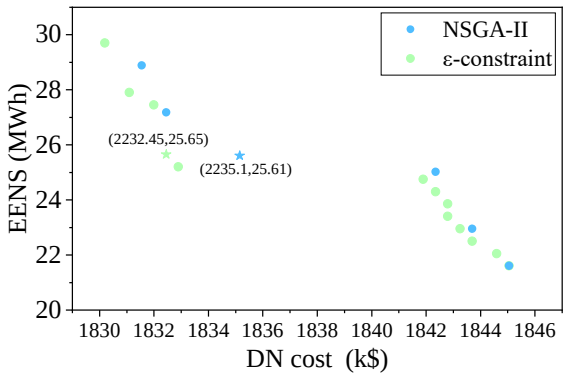

Fig. 9. Pareto front identified by NSGA-II and the ε-constraint method.

shedding associated with VSC failures, thereby enhancing the overall reliability of the system.

Figure 10(b) depicts the effects of variations in the proportion of DC components (including DC loads and DCDG) on system economy and reliability. As the proportion of DC components increases, the system cost initially rises before subsequently declining, while EENS exhibits a consistent upward trend. The analysis indicates that in systems composed solely of AC components, optimal planning can yield the lowest costs and highest reliability. However, an increase in the proportion of DC components leads to an increase in both cost and EENS for the optimal solution. It is important to note that if the system is exclusively designed for DC loads and distributed DC generation, there is a significant reduction in costs, although EENS experiences a slight increase. This observation underscores the considerable influence of high investment costs associated with energy converters on the overall system, as well as the diminished reliability of DC equipment due to elevated failure rates. The study concludes that investment in DC equipment becomes justifiable only when the proportion of DC components reaches a certain threshold, effectively balancing cost and reliability.

Figure 10(c) illustrates the effects of equipment failure rates on the reliability metrics associated with optimal planning solutions. A reduction in the failure rate of the VSC leads to a marked improvement in reliability indices, specifically SAIDI, SAIFI, and EENS, all of which exhibit a decrease. Consequently, further reductions in the failure rate are instrumental in enhancing the overall reliability of the system. This finding emphasizes the substantial influence of fault occurrences on system reliability, thereby underscoring the necessity for ongoing initiatives aimed at minimizing faults and enhancing system performance.

4.4 Discussion for Practical Application

Our study offers significant practical implications by presenting a ADHDN planning model that achieves balanced optimization between system economy and reliability, enabling planners to flexibly select solutions based on specific cost tolerances or reliability requirements, thereby significantly reducing overall costs while maintaining low reliability losses. It indicates that transitioning to DC systems is more rational when buses face significant DC loads or have a higher proportion of DC distributed generation resources, offering utilities clear criteria for technology selection under certain load structures and resource conditions. Furthermore, the adaptive ε-constraint method enhances computational efficiency and accuracy, allowing for faster acquisition of high-quality Pareto frontiers crucial for timely decision-making in dynamic power systems. Sensitivity analysis reveals that increasing the penetration rate of distributed generation decreases system costs and improves reliability metrics such as EENS, with an optimal proportion of DC elements where investment in DC equipment becomes reasonable, balancing cost and reliability. Lastly, our study highlights the potential application of ADHDN planning in configurations with a high proportion of DC systems, providing effective strategies for distribution systems containing numerous DC components, which are invaluable for modernizing existing grids or designing new ones with advanced technologies, ensuring better economic performance and enhanced reliability.

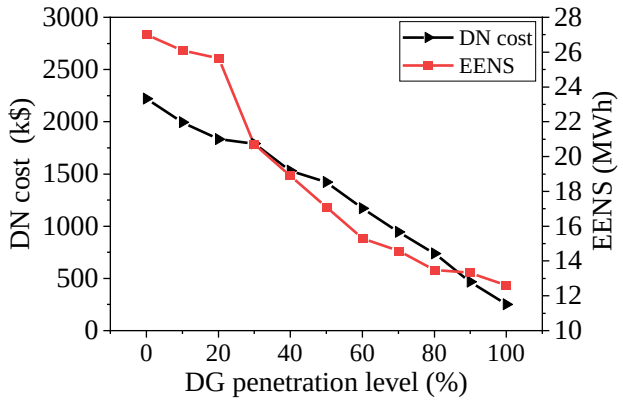

(a) Economic and reliability metrics versus DG penetration level

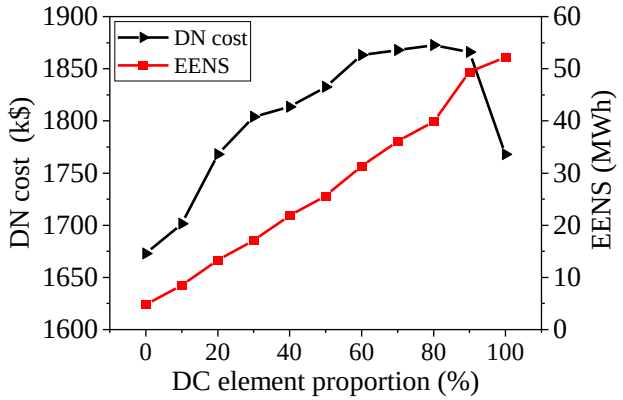

(b) Economic and reliability metrics versus DC element proportion

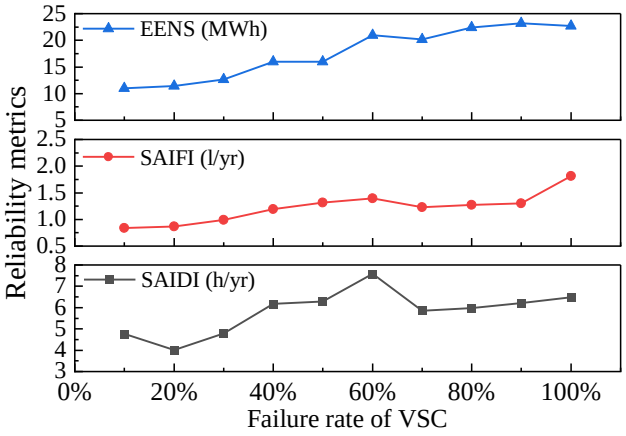

(c) Reliability metrics versus failure rate of VSC

Fig. 10. Changes of economic and reliability metrics with different DG penetration levels, DC element proportions and failure rates of VSC.

5. Conclusion

This study addresses the integration of explicit topology-based reliability assessment and ADHDN planning

problems, exploring modeling and algorithmic solution pathways. By integrating topology-related reliability quantification metrics with ADHDN power flow equations and implementing linearization, we propose an adaptive ε-constraint algorithm to effectively solve and present the global Pareto frontier.

The main findings of this study are as follows: 1) The proposed ADHDN planning model achieves an effective balance between system economy and reliability, realizing optimization configurations for dual objectives. Case study results demonstrate that the Pareto frontier of ADHDN planning surpasses the performance of single ACDN or DCDN models, exhibiting a broader range of preferred strategic options. In-depth analysis based on decision support techniques further confirms that ADHDN can significantly reduce the overall cost of the distribution system while maintaining low reliability losses. 2) Through the adaptive ε-constraint method, the solution of the double Q ADHDN planning model is not only efficient but also ensures the accuracy of the solutions, providing distribution system planners with a rich selection of options for planning under specific cost and reliability requirements. 3) Sensitivity analysis results reveal the potential application of ADHDN planning in configurations with a high proportion of DC systems, indicating its ability to provide effective planning strategies for distribution systems containing a large number of DC components.

Future work will expand this research to include more complex network topologies and emerging technologies like advanced energy storage and smart grid components. Researchers will also explore real-time optimization methods to improve the dynamic adaptability of ADHDN planning, as well as integrate artificial intelligence techniques to enhance predictive modeling and decision-making in power distribution networks. These efforts aim to advance the practical applicability and robustness of ADHDN planning methodologies.

Acknowledgment

This research was supported by the “Research on reliability planning technology of full voltage level distribution network based on multi-level collaboration” (Project No. 031000QQ00230007).

References

[1] YU, X., LI, W., MALEKI, A., et al. Selection of optimal location and design of a stand-alone photovoltaic scheme using a modified hybrid methodology. *Sustainable Energy Technologies and Assessments*, 2021, vol. 45, p. 1–15. DOI: 10.1016/j.seta.2021.101071

[2] AHMADIAN, A., SEDGHI, M., MOHAMMADI-IVATLOO, B., et al. Cost-benefit analysis of V2G implementation in distribution networks considering PEVs battery degradation. *IEEE Transactions on Sustainable Energy*, 2018, vol. 9, no. 2, p. 961 to 970. DOI: 10.1109/TSTE.2017.2768437

[3] CHEN, Y., SHI, K., CHEN, M., et al. Data center power supply systems: From grid edge to point-of-load. *IEEE Journal of Emerging and Selected Topics in Power Electronics*, 2023, vol. 11, no. 3, p. 2441–2456. DOI: 10.1109/JESTPE.2022.3229063

[4] ELSAYED, A. T., MOHAMED, A. A., MOHAMMED, O. A. DC microgrids and distribution systems: An overview. *Electric Power Systems Research*, 2015, vol. 119, p. 407–417. DOI: 10.1016/j.epsr.2014.10.017

[5] GHADIRI, A., HAGHIFAM, M. R., MIRI LARIMI, S. M. Comprehensive approach for hybrid AC/DC distribution network planning using genetic algorithm. *IET Generation, Transmission & Distribution*, 2017, vol. 11, no. 16, p. 3892–3902. DOI: 10.1049/iet-gtd.2016.1293

[6] RASTGOU, A. Distribution network expansion planning: An updated review of current methods and new challenges. *Renewable and Sustainable Energy Reviews*, 2024, vol. 189, p. 1–21. DOI: 10.1016/j.rser.2023.114062

[7] JOOSHAKI, M., ABBASPOUR, A., FOTUHI-FIRUZABAD, M., et al. An enhanced MILP model for multistage reliability-constrained distribution network expansion planning. *IEEE Transactions on Power Systems*, 2022, vol. 37, no. 1, p. 118–131. DOI: 10.1109/TPWRS.2021.3098065

[8] LI, Z., WU, W., TAI, X., et al. A reliability-constrained expansion planning model for mesh distribution networks. *IEEE Transactions on Power Systems*, 2021, vol. 36, no. 2, p. 948–960. DOI: 10.1109/TPWRS.2020.3015061

[9] PINTO, R. S., UNSIHUAY-VILA, C., TABARRO, F. H. Reliability-constrained robust expansion planning of active distribution networks. *IET Generation, Transmission & Distribution*, 2022, vol. 16, no. 1, p. 27–40. DOI: 10.1049/gtd2.12263

[10] LEE WILLIS, H. *Power Distribution Planning Reference Book*. 1st ed. Boca Raton: CRC Press, 2004. ISBN 9780429164798 DOI: 10.1201/9780824755386

[11] SIVANAGARAJU, S., RAO, J. V., RAJU, P. S. Discrete particle swarm optimization to network reconfiguration for loss reduction and load balancing. *Electric Power Components and Systems*, 2008, vol. 36, no. 5, p. 513–524. DOI: 10.1080/15325000701735389

[12] RUIZ-RODRIGUEZ, F. J., HERNÁNDEZ, J. C., JURADO, F. Voltage unbalance assessment in secondary radial distribution networks with single-phase photovoltaic systems. *International Journal of Electrical Power & Energy Systems*, 2015, vol. 64, p. 646–654. DOI: 10.1016/j.ijepes.2014.07.071

[13] RUIZ-RODRIGUEZ, F. J., GOMEZ-GONZALEZ, M., JURADO, F. Optimization of radial systems with biomass fueled gas engine from a metaheuristic and probabilistic point of view. *Energy Conversion and Management*, 2013, vol. 65, p. 343–350. DOI: 10.1016/j.enconman.2012.09.002

[14] GOMEZ-GONZALEZ, M., LÓPEZ, A., JURADO, F. Optimization of distributed generation systems using a new discrete PSO and OPF. *Electric Power Systems Research*, 2012, vol. 84, no. 1, p. 174–180. DOI: 10.1016/j.epsr.2011.11.016

[15] BAGHERI, A., MONSEF, H., LESANI, H. Integrated distribution network expansion planning incorporating distributed generation considering uncertainties, reliability, and operational conditions. *International Journal of Electrical Power & Energy Systems*, 2015, vol. 73, p. 56–70. DOI: 10.1016/j.ijepes.2015.03.010

[16] BORGES, C. L. T., MARTINS, V. F. Multistage expansion planning for active distribution networks under demand and Distributed Generation uncertainties. *International Journal of Electrical Power & Energy Systems*, 2012, vol. 36, no. 1, p. 107 to 116. DOI: 10.1016/j.ijepes.2011.10.031

[17] MUÑOZ-DELGADO, G., CONTRERAS, J., ARROYO, J. M. Multistage generation and network expansion planning in distribution systems considering uncertainty and reliability. *IEEE*

Transactions on Power Systems, 2016, vol. 31, no. 5, p. 3715 to 3728. DOI: 10.1109/TPWRS.2015.2503604

[18] POMBO, A. V., MURTA-PINA, J., PIRES, V. F. A multiobjective placement of switching devices in distribution networks incorporating distributed energy resources. *Electric Power Systems Research*, 2016, vol. 130, p. 34–45. DOI: 10.1016/j.epsr.2015.08.012

[19] LI, Z., WU, W., ZHANG, B., et al. Analytical reliability assessment method for complex distribution networks considering post-fault network reconfiguration. *IEEE Transactions on Power Systems*, 2020, vol. 35, no. 2, p. 1457–1467. DOI: 10.1109/TPWRS.2019.2936543

[20] TABARES, A., MUÑOZ-DELGADO, G., FRANCO, J. F., et al. An enhanced algebraic approach for the analytical reliability assessment of distribution systems. *IEEE Transactions on Power Systems*, 2019, vol. 34, no. 4, p. 2870–2879. DOI: 10.1109/TPWRS.2019.2892507

[21] LI, J., KONG, H., WANG, W., et al. A novel reliability assessment method for distribution networks based on linear programming considering distribution automation and distributed generation. *IET Renewable Power Generation*, 2024, vol. 18, no. 3, p. 529–544. DOI: 10.1049/rpg2.12818

[22] MANSOURI, S. A., NEMATBAKHSH, E., AHMARINEJAD, A., et al. A hierarchical scheduling framework for resilience enhancement of decentralized renewable-based microgrids considering proactive actions and mobile units. *Renewable and Sustainable Energy Reviews*, 2022, vol. 168, p. 1–23. DOI: 10.1016/j.rser.2022.112854

[23] TABARES, A., MUÑOZ-DELGADO, G., FRANCO, J. F., et al. Multistage reliability-based expansion planning of ac distribution networks using a mixed-integer linear programming model. *International Journal of Electrical Power & Energy Systems*, 2022, vol. 138, p. 1–12. DOI: 10.1016/j.ijepes.2021.107916

[24] ALANAZI, M., ALANAZI, A., AKBARI, M. A., et al. A non-simulation-based linear model for analytical reliability evaluation of radial distribution systems considering renewable DGs. *Applied Energy*, 2023, vol. 342, p. 1–11. DOI: 10.1016/j.apenergy.2023.121153

[25] WEI, W., ZHOU, Y., ZHU, J., et al. Reliability assessment for AC/DC hybrid distribution network with high penetration of renewable energy. *IEEE Access*, 2019, vol. 7, p. 153141–153150. DOI: 10.1109/ACCESS.2019.2947707

[26] XU, X., TAI, N., HU, Y., et al. Reliability calculation of AC/DC hybrid distribution network with a solid-state transformer. *The Journal of Engineering*, 2019, vol. 2019, no. 16, p. 3067–3071. DOI: 10.1049/joe.2018.8385

[27] WU, T., WANG, J., LU, X., et al. AC/DC hybrid distribution network reconfiguration with microgrid formation using multi-agent soft actor-critic. *Applied Energy*, 2022, vol. 307, p. 1–11. DOI: 10.1016/j.apenergy.2021.118189

[28] MUÑOZ-DELGADO, G., CONTRERAS, J., ARROYO, J. M. Joint expansion planning of distributed generation and distribution networks. *IEEE Transactions on Power Systems*, 2015, vol. 30, no. 5, p. 2579–2590. DOI: 10.1109/TPWRS.2014.2364960

[29] MAVROTAS, G., FLORIOS, K. An improved version of the augmented ε-constraint method (AUGMECON2) for finding the exact Pareto set in multi-objective integer programming problems. *Applied Mathematics and Computation*, 2013, vol. 219, no. 18, p. 9652–9669. DOI: 10.1016/j.amc.2013.03.002

[30] AHMED, H. M. A., ELTANTAWY, A. B., SALAMA, M. M. A. A reliability-based stochastic planning framework for AC-DC hybrid smart distribution systems. *International Journal of Electrical Power & Energy Systems*, 2019, vol. 107, p. 10–18. DOI: 10.1016/j.ijepes.2018.11.003

[31] MAVROTAS, G. Effective implementation of the ε-constraint method in multi-objective mathematical programming problems. *Applied Mathematics and Computation*, 2009, vol. 213, no. 2, p. 455–465. DOI: 10.1016/j.amc.2009.03.037

About the Authors ...

Jianjian JIANG was born in Changsha, Hunan, China. He received his Ph.D. degree from Tsinghua University in 2004. His research interests include power network planning and power supply reliability studies.

Qiang LUO was born in Ziyang, Sichuan, China. He received his M.Sc. degree from Huazhong University of Science and Technology in 2019. His research interests include distribution network planning.

Zhiheng XU was born in Zhanjiang, Guangdong, China. He received his M.Sc. degree from South China University of Technology in 2018. His research interests include distribution network planning.

Hao LI was born in Yiyang, Hunan, China. He received his M.Sc. degree from Huazhong University of Science and Technology in 2017. His research interests include distribution network planning and power supply reliability studies.

Chong GAO was born in Jixi, Heilongjiang, China. He received his M.Sc. degree from North China Electric Power University in 2008. His research interests include distribution network planning.